Gauss Quadrature Approximations to Hypergeometric and Confluent Hypergeometric Functions

WALTER GAUTSCHI

ABSTRACT. Integral representations of hypergeometric and confluent hypergeometric functions with real parameters and complex arguments are used to approximate these functions by Gaussian quadrature. An analysis is given of the errors involved and of estimates of the number of Gauss points required to achieve any given accuracy. Numerical examples illustrate the theory.

0. Introduction

Hypergeometric and confluent hypergeometric functions admit integral representations for parameter values restricted by certain inequalities. Applying Gaussian quadrature to these integrals produces approximations valid in the whole complex plane, for the confluent hypergeometric function, and in the whole complex plane cut along the segment $[1, \infty]$ of the positive real axis, for the hypergeometric function. The former are studied in §1. Numerical evidence, graphically displayed, demonstrates the effectiveness of these quadrature approximations. The error is analyzed both in terms of derivatives of the integrand (in the case of the confluent hypergeometric function) and in terms of derivative-free contour integral representations of the remainder term. Both approaches lead to a priori estimates of the number of Gauss points needed for given accuracy. Analogous analyses are given in §2 for the hypergeometric function. The paper ends with §3 containing some concluding remarks.

1. Confluent Hypergeometric Functions

1.1. *Quadrature approximation.* Our interest is in the confluent hypergeometric function $M(a, b; z)$, also known as Kummer's function, when a and b are positive parameters satisfying $b > a > 0$ and z is real or complex. One then has the well-known integral representation (see, e.g. Abramowitz and Stegun [1, Eq.**13.2.1**])

$$M(a, b; z) = \frac{\Gamma(b)}{\Gamma(a)\Gamma(b-a)} \int_0^1 e^{zt} w_{a,b}(t)dt, \tag{1.1}$$

where

$$w_{a,b}(t) = (1-t)^{b-a-1} t^{a-1} \tag{1.2}$$

is a Jacobi weight function on the interval $[0, 1]$ with Jacobi parameters $\alpha = b - a - 1$, $\beta = a - 1$. We propose to approximate the integral in (1.1) by an n-point Gauss-Jacobi quadrature rule

$$\int_0^1 e^{zt} w_{a,b}(t)dt = \sum_{k=1}^{n} w_k^J e^{zt_k^J} + E_n(a, b; z), \tag{1.3}$$

where t_k^J and w_k^J are the Gauss-Jacobi nodes and weights for the interval $[0, 1]$ (rather than the standard interval $[-1, 1]$). These quadrature rules, after the change of variables $t \mapsto \frac{1}{2}(1 + t)$, are readily generated by the software provided in [6].

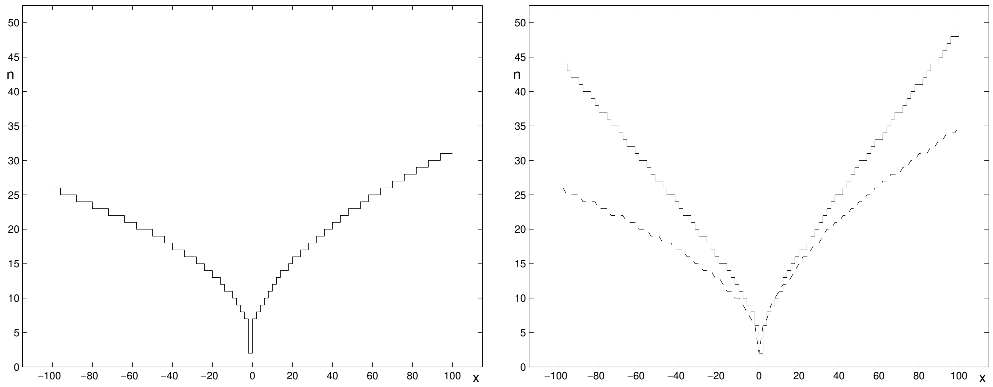

Figure 1.1. Values of n of n-point quadrature rules (1.3) yielding 10-digit accuracy for real arguments z; left: experimentally determined, right: estimated

1.2. *Numerical data.* The approximation (1.3) clearly converges as $n \to \infty$ for any complex z, since the integrand is continuous on $[0,1]$, in fact an entire function of t. With regard to the quality of convergence, we first describe some numerical tests.

We experimentally determined the smallest value of n that, for given a, b, and z, yields a prescribed relative accuracy ε (absolute accuracy ε if the result is less than 1 in absolute value). The left frame of Figure 1.1 shows the maximum of this smallest n as a function of real $z = x$, $-100 \le x \le 100$, where the maximum is taken over $a = .25(.25)5$, $b = (a + .25)(.25)5$ and $\varepsilon = \frac{1}{2} \times 10^{-10}$. The right frame displays the analogous n as estimated below in (1.9), (1.24) (and modified as described in the last paragraph of §1.4). It is seen that for real $z = x$ in $[-100, 100]$ and 10-digit accuracy, a Gauss rule of not more than 30 points will do, the case $x < 0$ being slightly more favorable than the case $x > 0$. Note also that for real $z = x$, the quadrature sum in (1.3) consists of positive terms only, so that its evaluation is perfectly stable.

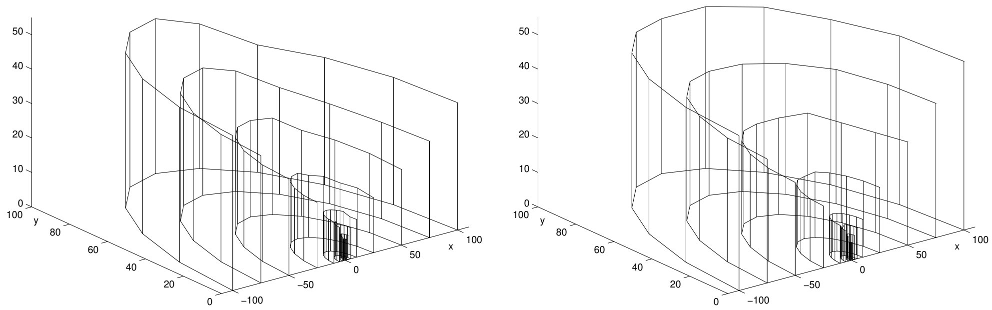

Figure 1.2. Values of n of n-point quadrature rules yielding 10-digit accuracy for complex arguments z; left: experimentally determined, right: estimated

Analogous values of n — experimental and estimated via (1.9) below — for complex $z = re^{i\varphi}$, $0 < r \le 100$, $0 \le \varphi \le \pi$, are depicted in Fig. 1.2. Here, a 50-point Gauss rule will suffice.

1.3. *Error estimates in terms of derivatives.* If $u(t)$ and $v(t)$ denote the real and imaginary parts of e^{zt}, one has from the well-known error formula for Gaussian quadrature [2, Theorem, p. 98], applied separately to the real and imaginary part of (1.3),

$$E_n(a, b; z) = \frac{1}{(2n)!}\,[u^{(2n)}(\tau_u) + iv^{(2n)}(\tau_v)]\gamma_n(a, b), \tag{1.4}$$

where

$$\gamma_n(a,b) = \int_0^1 [\pi_n(t; w_{a,b})]^2 w_{a,b}(t)dt.$$

Here, $\pi_n(\,\cdot\,; w_{a,b})$ is the monic Jacobi polynomial relative to the interval $[0,1]$ (the polynomial $G_n(b-1,a,t)$ in the notation of [1, Table **22.2**]), and τ_u, τ_v are certain numbers between 0 and 1. From [1, Table **22.2**] one has

$$\gamma_n(a,b) = \frac{n!\Gamma(n+a)\Gamma(n+b-1)\Gamma(n+b-a)}{(2n+b-1)\Gamma^2(2n+b-1)}.$$

For $n=0$, the quantity γ_0 is just the reciprocal of the numerical factor multiplying the integral in (1.1); thus,

$$M(a,b;z) = \frac{1}{\gamma_0(a,b)} \int_0^1 e^{zt} w_{a,b}(t)dt. \tag{1.1$'$}$$

Using Stirling's formula for the gamma function, one finds, after straightforward computation,

$$\gamma_n(a,b) \sim \frac{\pi}{2^{2b-3}}\, 2^{-4n}, \quad n \to \infty. \tag{1.5}$$

On the other hand, letting $z = x+iy = re^{i\varphi}$, one has

$$\frac{d^{2n}}{dt^{2n}}\, e^{zt} = z^{2n}e^{zt} = r^{2n}e^{xt+i(yt+2n\varphi)},$$

so that

$$|u^{(2n)}(t)| \le r^{2n}e^{xt}, \quad |v^{(2n)}(t)| \le r^{2n}e^{xt}.$$

There follows from (1.4) that

$$|E_n(a,b;z)| \le \frac{\delta(y)\gamma_n(a,b)}{(2n)!}\,|z|^{2n}e_+^x, \tag{1.6}$$

where

$$\delta(y) = \begin{cases} 1 & \text{if } y=0, \\ 2 & \text{otherwise}, \end{cases} \qquad e_+^x = \begin{cases} 1 & \text{if } x \le 0, \\ e^x & \text{otherwise}, \end{cases}$$

or, asymptotically for $n \to \infty$, with the help of (1.5) and Stirling's formula for $(2n)!$,

$$|E_n(a,b;z)| \lesssim \sqrt{\frac{\pi}{n}}\,\frac{1}{2^{2b-3}}\,\left(\frac{e|z|}{8n}\right)^{2n} e_+^x. \tag{1.7}$$

Actually, if $y = 0$, the bound on the right could be halved, but this is of little consequence. It is interesting to note that the error bound in (1.7) does not depend on a, and could be made independent of b as well by letting $b = 0$.

1.4. *Estimate of n for prescribed accuracy.* In order to estimate the number n of Gauss points needed to achieve an error tolerance $\varepsilon > 0$, we disregard the factor $\sqrt{\pi/n}$ in (1.7) and note that $|E_n| \leq \varepsilon$ if

$$\left(\frac{e|z|}{8n}\right)^{2n} \leq \frac{2^{2b-3}}{e_+^x}\,\varepsilon$$

or, equivalently,

$$\frac{8n}{e|z|}\ln\frac{8n}{e|z|} \geq \frac{4}{e|z|}\left\{x_+ + (3-2b)\ln 2 + \ln\frac{1}{\varepsilon}\right\}, \tag{1.8}$$

where $x_+ = x$ if $x \geq 0$ and $x_+ = 0$ if $x < 0$. Denoting by $t(s)$ the inverse function of $s = t\ln t$, one has $t\ln t \geq c$, $c \geq 0$, if and only if $t \geq t(c)$. Hence, (1.8) can be given the form

$$n \geq \frac{e|z|}{8}\cdot t\left(\frac{4}{e|z|}[x_+ + (3-2b)\ln 2 + \ln\frac{1}{\varepsilon}]\right). \tag{1.9}$$

Low-accuracy approximations of the function $t(s)$ are given in Gautschi [5, pp. 51–52].

The analysis given here is aimed towards attaining a given *absolute* error in (1.3), not relative error. In practice, however, it is usually the relative error that one wants to control, i.e., the relative error

$$\frac{M(a,b;z) - \dfrac{1}{\gamma_0(a,b)}\displaystyle\sum_{k=1}^{n} w_k^J e^{zt_k^J}}{M(a,b;z)} = \frac{E_n(a,b;z)}{\displaystyle\int_0^1 e^{zt}w_{a,b}(t)dt}.$$

This is particularly so if $|M(a,b;z)| > 1$. (Otherwise, control of the absolute error is often adequate.) Thus, we want

$$|E_n(a,b;z)| \leq \varepsilon\left|\int_0^1 e^{zt}w_{a,b}(t)dt\right| \quad \text{if} \quad \left|\int_0^1 e^{zt}w_{a,b}(t)dt\right| > \gamma_0,$$

and

$$|E_n(a,b;z)| \le \varepsilon\gamma_0 \quad \text{if} \quad \left| \int_0^1 e^{zt} w_{a,b}(t)dt \right| \le \gamma_0.$$

While this would seem to require knowledge of the integral, a rough estimate of it suffices. Once in possession of such an estimate, one can simply apply the formula for n in (1.9), but replace ε respectively by ε multiplied by the absolute value of that estimate, or by $\varepsilon\gamma_0$. The estimate in question can be obtained, e.g., by applying a low-order Gaussian quadrature rule to the integral in (1.1). Extensive tests have shown that a 10-point rule should be adequate for this purpose. The solid graph in the right frame of Fig. 1.1 displays the estimate of n so obtained.

1.5. *Derivative-free error estimates.* The change of variables $t \mapsto \frac{1}{2}(1+t)$ transforms the integral in (1.1) into one over $[-1,1]$,

$$M(a,b;z) = \frac{1}{\gamma_0^J(a,b)} \int_{-1}^1 e^{\frac{1}{2}z(1+t)} w_{a,b}^J(t)dt. \tag{1.10}$$

Here, γ_0^J, and more generally, γ_n^J, are the normalization factors of the standard (monic) Jacobi polynomials,

$$\gamma_n^J(a,b) = \int_{-1}^1 [\pi_n^J(t; w_{a,b}^J)]^2 w_{a,b}^J(t)dt, \tag{1.11}$$

where

$$w_{a,b}^J(t) = (1-t)^{b-a-1}(1+t)^{a-1}.$$

The error term of the n-point Gauss-Jacobi quadrature rule applied to the integral in (1.10) will be denoted by $E_n^J(a,b;z)$, and the integrand by

$$f^J(t;z) = e^{\frac{1}{2}z(1+t)}. \tag{1.12}$$

A derivative-free estimate of E_n^J is given by (see, e.g., [7])

$$E_n^J(a,b;z) = \frac{1}{2\pi i} \oint_\Gamma K_n(\zeta) f^J(\zeta;z)d\zeta, \tag{1.13}$$

where for Γ one may take a circle $\Gamma = C_R$ of radius $R > 1$ centered at the origin. The "kernel" K_n of the quadrature error can be represented, e.g., by

$$K_n(\zeta) = \frac{\rho_n(\zeta)}{\pi_n(\zeta)}, \tag{1.14}$$

where $\pi_n(\zeta) = \pi_n(\zeta; w^J_{a,b})$ is the monic Jacobi polynomial belonging to the weight function $w^J_{a,b}$, and

$$\rho_n(\zeta) = \rho_n(\zeta; w^J_{a,b}) = \int_{-1}^{1} \frac{\pi_n(t)}{\zeta - t}\, w^J_{a,b}(t)dt, \quad \zeta \in \mathbb{C}\backslash[-1,1].$$

The kernel tends to 0 as $n \to \infty$ for any complex $\zeta \notin [-1,1]$, the faster the further away ζ is from the interval $[-1,1]$. It is easily computed by recursion (see [7, §4]), provided ζ is not too close to $[-1,1]$. From [7, §3] it follows, moreover, that

$$\max_{\zeta \in C_R} |K_n(\zeta)| = \begin{cases} K_n(R) & \text{if } b \le 2a, \\ K_n(-R) & \text{if } b > 2a. \end{cases} \tag{1.15}$$

Consequently, by (1.13),

$$|E^J_n(a,b;z)| \le |RK_n(\pm R)| \cdot \max_{\zeta \in C_R} |f^J(\zeta; z)|, \tag{1.16}$$

where the plus or minus sign holds according as $b \le 2a$ or $b > 2a$. The maximum on the right is easily found to be

$$\max_{\zeta \in C_R} |f^J(\zeta; z)| = e^{\frac{1}{2}r(R+\cos\varphi)}, \tag{1.17}$$

where, as before, $z = re^{i\varphi}$. Thus,

$$|E^J_n(a,b;z)| \le |RK_n(\pm R)| \cdot e^{\frac{1}{2}r(R+\cos\varphi)}. \tag{1.18}$$

This holds for any $R > 1$. Optimizing the bound then yields

$$|E^J_n(a,b;z)| \le \min_{R>1}\{|RK_n(\pm R)| \cdot e^{\frac{1}{2}r(R+\cos\varphi)}\}, \quad z = re^{i\varphi}. \tag{1.19}$$

In the numerical work described below, the kernel K_n has been computed by means of the double-precision routine `dkern` of [6]. (It calls for the additional routines `d1mach`, `drecur`, `nu0jac`, and `dknum`.)

Table 1.1 illustrates this bound for $a = .5$ and $b = 2.5$. For each n and $r = |z|$, there are four entries. The two upper ones are bounds for the relative error when $\varphi = 0$ and absolute error when $\varphi = \pi$. The two lower ones are the optimal values of R that yield the minimum in (1.19) for these two values

n	5	5	10	10	20	20	50	50
r	$\varphi = 0$	$\varphi = \pi$	$\varphi = 0$	$\varphi = \pi$	$\varphi = 0$	$\varphi = \pi$	$\varphi = 0$	$\varphi = \pi$
1	.19e–11	.87e–12	.35e–29	.16e–29	.13e–70	.60e–71	.13e–216	.61e–217
	20.2	20.2	40.1	40.1	80.1	80.0	200.	200.
5	.43e–4	.18e–5	.64e–15	.26e–16	.20e–42	.82e–44	.17e–146	.68e–148
	4.26	4.26	8.14	8.14	16.1	16.1	40.0	40.0
10	.38e–1	.33e–3	.40e–9	.34e–11	.11e–30	.92e–33	.90e–117	.77e–119
	2.37	2.37	4.20	4.20	8.10	8.10	20.0	20.0
20	.11e+2	.21e–1	.43e–4	.85e–7	.66e–20	.12e–22	.43e–88	.85e–91
	1.51	1.51	2.30	2.30	4.16	4.16	10.1	10.1
50	.29e+4	.88e+0	.46e+1	.14e–2	.41e–8	.13e–11	.24e–53	.75e–57
	1.12	1.12	1.33	1.33	1.92	1.92	4.14	4.14
100	.65e+5	.50e+1	.17e+4	.13e+0	.92e–2	.70e–6	.23e–31	.17e–35
	1.04	1.04	1.10	1.10	1.30	1.30	2.25	2.25

TABLE 1.1 Optimized error bounds for $a = .5$, $b = 2.5$

of φ. According to the discussion at the end of §1.4, bounds for the relative resp. absolute error are obtained by dividing the bound in (1.19) respectively by $\gamma_0^J M(a, b; r)$ and by γ_0^J, since for $\varphi = 0$ and $\varphi = \pi$ one has respectively $M(a, b, r) > 1$ and $M(a, b; -r) < 1$. It is seen that the errors for $\varphi = \pi$ are consistently smaller than those for $\varphi = 0$, confirming what was experimentally observed in the left frame of Fig. 1.1. Evidently, the reason for this is the presence of the term $\cos\varphi$ in the exponential on the right of (1.19).

Comparing the error bounds in Table 1.1 with error bounds derivable from (1.7), one finds general agreement within 1 to 2 orders of magnitude when $r = 1$, 5, or 10. For larger values of r, however, the bounds in Table 1.1 become progressively better, by as much as 17 orders of magnitude (when $r = 100$ and $n = 50$).

1.6. *Asymptotics for* $K_n(\pm R)$. If $K_n^{(\alpha,\beta)}(\zeta) = \rho_n^{(\alpha,\beta)}(\zeta)/\pi_n^{(\alpha,\beta)}(\zeta)$ denotes the kernel (1.14) for the Jacobi weight function $(1-t)^\alpha(1+t)^\beta$, it is known (see [4], [3, Appendix A.1]) that, for ζ away from $[-1, 1]$,

$$K_n^{(\alpha,\beta)}(\zeta) \sim c_n(\alpha, \beta)\, \frac{(\zeta-1)^\alpha(\zeta+1)^\beta}{(\zeta+\sqrt{\zeta^2-1})^{2n+\alpha+\beta+1}}, \qquad n \to \infty, \tag{1.20}$$

where $-\pi < \arg(\zeta \pm 1) < \pi$ and

$$c_n(\alpha, \beta) = 2^{4n+2(\alpha+\beta+1)}\, \frac{\Gamma(n+\alpha+1)\Gamma(n+\beta+1)\Gamma(n+1)\Gamma(n+\alpha+\beta+1)}{\Gamma(2n+\alpha+\beta+2)\Gamma(2n+\alpha+\beta+1)}.$$

Applying Stirling's formula to the gamma functions above yields

$$c_n(\alpha,\beta) \sim 2\pi. \tag{1.21}$$

We need (1.20) for real $\zeta = R$ and $\zeta = -R$, $R > 1$. From the well-known property of Jacobi polynomials $\pi_n^{(\alpha,\beta)}(-\zeta) = (-1)^n \pi_n^{(\beta,\alpha)}(\zeta)$, which implies $\rho_n^{(\alpha,\beta)}(-\zeta) = -\rho_n^{(\beta,\alpha)}(\zeta)$, one obtains from (1.20), (1.21), as $n \to \infty$,

$$|K_n^{(\alpha,\beta)}(\pm R)| \sim 2\pi \frac{|\pm R - 1|^\alpha \, |\pm R + 1|^\beta}{(R + \sqrt{R^2-1})^{2n+\alpha+\beta+1}}, \quad R > 1. \tag{1.22}$$

Inserting this into (1.19), with $\alpha = b - a - 1$, $\beta = a - 1$, one gets

$$|E_n^J(a,b;z)| \lesssim \min_{R>1} \left\{ 2\pi \frac{R\,|\pm R - 1|^{b-a-1} \, |\pm R + 1|^{a-1}}{(R + \sqrt{R^2-1})^{2n+b-1}} \cdot e^{\frac{1}{2} r (R + \cos\varphi)} \right\}, \quad z = re^{i\varphi}. \tag{1.23}$$

Using this bound in place of the one in (1.19), we reproduced Table 1.1 and found almost perfect agreement. (The largest discrepancy observed was 2 units in the second decimal digit of the mantissas.)

It is also possible to estimate n such that $|E_n^J(a,b;z)| \le \varepsilon$ by combining (1.22) with (1.18). One finds

$$n \ge \frac{1}{2}\left(1 - b + \min_{R>1} \frac{\frac{1}{2} r (R + \cos\varphi) + \ln(2\pi R\,|\pm R - 1|^{b-a-1} |\pm R + 1|^{a-1}) + \ln\frac{1}{\varepsilon}}{\ln(R + \sqrt{R^2-1})}\right). \tag{1.24}$$

The minimum on the right is best obtained numerically, by evaluating the objective function at the zero of its derivative (and making sure that it is indeed a minimum).

The dashed graph in the right frame of Fig. 1.1 shows the estimate of n as obtained from (1.24) with $z = re^{i\varphi}$, $\varphi = 0$ and $\varphi = \pi$, when ε is modified as discussed at the end of §1.4.

2. Hypergeometric Functions

2.1. *Quadrature approximation.* We now consider the hypergeometric function $F(a,b;c;z)$, for real parameters a and $c > b > 0$, and real or complex z in the complex plane cut along the line from 1 to ∞. We will assume throughout that $z \ne 0$, since otherwise one trivially has $F(a,b;c;0) = 1$. The integral representation then is (cf. Abramowitz and Stegun [1, Eq. **15.3.1**])

$$F(a,b;c;z) = \frac{\Gamma(c)}{\Gamma(b)\Gamma(c-b)} \int_0^1 (1 - zt)^{-a} w_{b,c}(t)\,dt, \tag{2.1}$$

where $w_{b,c}$ is the Jacobi weight (1.2) with a replaced by b, and b by c. The Gauss quadrature approximation of the integral in (2.1) is

$$\int_0^1 (1-zt)^{-a} w_{b,c}(t)dt = \sum_{k=1}^n w_k^J (1-zt_k^J)^{-a} + E_n(a,b;c;z), \tag{2.2}$$

the Jacobi nodes t_k^J and weights w_k^J now referring to the Jacobi weight function $w_{b,c}$. (The use of (2.2) was already suggested in 1955 by Karmazina [8], who provided tables of the Gauss nodes t_k^J and weights w_k^J for selected values of the parameters b and c, but gave no analysis of the error.) In analogy to (1.1′), one has

$$F(a,b;c;z) = \frac{1}{\gamma_0(b,c)} \int_0^1 (1-tz)^{-a} w_{b,c}(t)dt. \tag{2.1′}$$

2.2. *Numerical data.* The Gauss quadrature approximation in (2.2) converges for any z in the complex plane cut along $[1,\infty]$, since the integrand then is a continuous function of t. However, the error analysis given for the confluent hypergeometric function in §§1.3 and 1.4 does not carry over. The reason is that the $2n$th derivative of the integrand now is

$$\frac{d^{2n}}{dt^{2n}}(1-zt)^{-a} = (a)_{2n}(1-zt)^{-a-2n} z^{2n}, \tag{2.3}$$

with $(a)_{2n} = a(a+1)\cdots(a+2n-1)$ the Pochhammer symbol. The latter behaves like $(2n)!$ for large n, which cancels the $(2n)!$ in the denominator of the error formula analogous to (1.4). What remains, in spite of the rapid decrease of $\gamma_n(b,c)$, will no longer necessarily tend to zero as $n \to \infty$. The derivative-free error estimation of §1.5, on the other hand, applies also in the present context if appropriately modified. Before discussing this, it may be useful to make some preliminary remarks and describe numerical tests.

A first observation that can be made is that the quadrature error $E_n(a,b;c;z)$ will behave differently depending on whether a is negative or positive. In the former case, the integrand

$$f(t;z) = (1-zt)^{-a} \tag{2.4}$$

of (2.1) is a "polynomial-like" function of t, and in fact an outright polynomial if a is a negative integer. Moreover, the Gauss formula (2.2) has zero error, $E_n(a,b;c;z) = 0$, if a is a nonpositive integer $a \geq -2n+1$. If a is negative

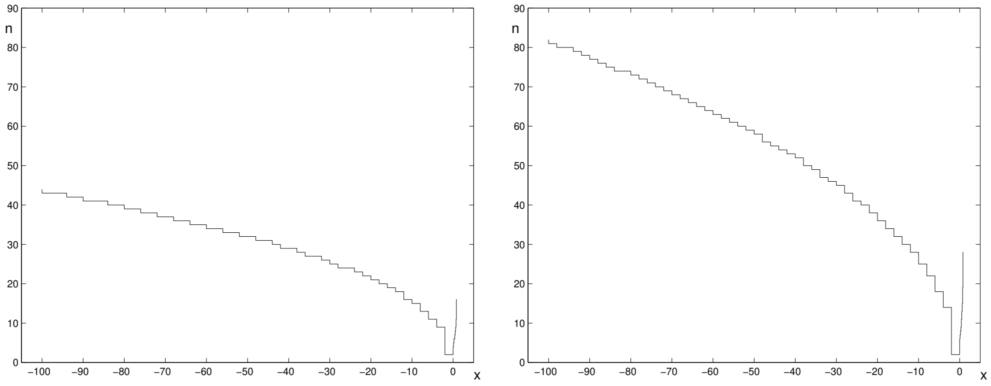

Figure 2.1. Values of n of n-point quadrature rules (2.2) yielding 10-digit accuracy for real arguments z; left: $a < 0$, right: $a > 0$

but not an integer, and z is on the cut $[1, \infty]$, then $f(t; z)$ has a branch-point singularity for some $t \in (0, 1]$, but remains bounded. None of this is true if a is positive. One therefore expects convergence of the Gauss formula (2.2) to be faster for negative values of a, and slower for positive values. This is borne out in the graphs of Fig. 2.1 for real $z = x$, $-100 \leq x < 1$, and in the graphs of Fig. 2.2 for complex $z = 1 + re^{i\varphi}$, $0 < r \leq 100$, $\pi \geq \varphi \geq \frac{1}{4}\pi$ (note the slightly different notation compared to the one in §1). In both figures the maximum values of n are shown that are required for 10-digit accuracy, the maximum being taken over $a = -5(.5)0$ resp. $a = .5(.5)5$. In either case,

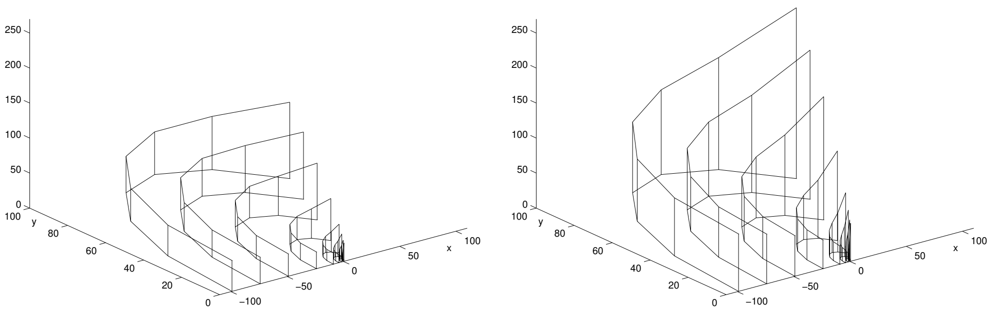

Figure 2.2. Values of n of n-point quadrature rules (2.2) yielding 10-digit accuracy for complex arguments z; left: $a < 0$, right: $a > 0$

one clearly needs considerably larger values of n to achieve a prescribed accuracy than is the case for confluent hypergeometric functions, and the situation gets worse as z approaches the cut $[1,\infty]$. (This is why we omitted φ-values between 0 and $\frac{1}{4}\pi$.)

2.3. *Derivative-free error estimates.* We make the same change of variables as at the beginning of §1.5, thus writing

$$F(a,b;c;z) = \frac{1}{\gamma_0^J(b,c)} \int_{-1}^{1} \left[1 - \tfrac{1}{2}z(1+t)\right]^{-a} w_{b,c}^J(t)dt. \tag{2.1''}$$

The integrand

$$f^J(t;z) = \left[1 - \tfrac{1}{2}z(1+t)\right]^{-a}, \quad z \in \mathbb{C}\backslash[1,\infty], \tag{2.5}$$

is holomorphic in the variable t in the whole complex plane cut along the line $\frac{\lambda}{z} - 1$, $\lambda \geq 2$. We shall denote this cut plane by $\mathbb{C}_z^*$. The cut lies entirely outside the unit circle if and only if $\left|\frac{\lambda}{z} - 1\right|^2 > 1$ for all $\lambda \geq 2$, which is easily seen to be equivalent to $\operatorname{Re} z < 1$. In this case, the method used in §1.5 to estimate the quadrature error still applies provided one takes circular contours about the origin with radii R satisfying $1 < R < \left|\frac{2}{z} - 1\right|$. Otherwise, a family of confocal ellipses (with foci at ± 1) can be used that are sufficiently slim to leave the cut outside. These, of course, can also be used in the former case. We discuss the two cases separately.

2.3.1. *The case* $\operatorname{Re} z < 1$. With $E_n^J(a,b;c;z)$ denoting the error term of Gauss-Jacobi quadrature applied to the integral in (2.1″), we have

$$E_n^J(a,b;c;z) = \frac{1}{2\pi i} \oint_\Gamma K_n(\zeta) f^J(\zeta;z)d\zeta. \tag{2.6}$$

Here, K_n is the same kernel as in (1.14), but with the parameters a, b replaced by b, c, respectively, and Γ is any contour encircling $[-1,1]$ and lying inside the cut plane $\mathbb{C}_z^*$. If $\Gamma = C_R$ with $1 < R < \left|\frac{2}{z} - 1\right|$, then, as in (1.16),

$$|E_n^J(a,b;c;z)| \leq |RK_n(\pm R)| \cdot \max_{\zeta \in C_R} |f^J(\zeta;z)|, \tag{2.7}$$

with the plus or minus sign holding according as $c \leq 2b$ or $c > 2b$. It remains to determine the maximum on the right.

Writing $z = x + iy$, $x < 1$ and $\zeta = Re^{i\theta}$, we have

$$|1 - \tfrac{1}{2}z(1+\zeta)| = h(\theta),$$
$$h^2(\theta) = 1 - x + \tfrac{1}{4}|z|^2(R^2+1) - R[(x - \tfrac{1}{2}|z|^2)\cos\theta - y\sin\theta],$$
$$0 \le \theta < 2\pi.$$

If we let

$$\mu_R^+(z) = \max_{\zeta \in C_R} |1 - \tfrac{1}{2}z(1+\zeta)|,$$
$$\mu_R^-(z) = \min_{\zeta \in C_R} |1 - \tfrac{1}{2}z(1+\zeta)|, \tag{2.8}$$

we have

$$[\mu_R^{\pm}(z)]^2 = 1 - x + \tfrac{1}{4}|z|^2(R^2+1) \pm R\sqrt{(x - \tfrac{1}{2}|z|^2)^2 + y^2},$$

which simplifies to

$$\mu_R^{\pm}(z) = \tfrac{1}{2}\,\big|\,|z-2| \pm R|z|\,\big|\,. \tag{2.9}$$

It follows from (2.5) that

$$\max_{\zeta \in C_R} |f^J(\zeta; z)| = \begin{cases} [\mu_R^+(z)]^{-a} & \text{if } a < 0, \\ [\mu_R^-(z)]^{-a} & \text{if } a > 0. \end{cases} \tag{2.10}$$

Combining (2.7) and (2.10), and optimizing the error bound at the same time, we get

$$|E_n^J(a,b;c;z)| \le \begin{cases} \min\limits_R |RK_n(\pm R)|\,[\mu_R^+(z)]^{-a} & \text{if } a < 0, \\ \min\limits_R |RK_n(\pm R)|\,[\mu_R^-(z)]^{-a} & \text{if } a > 0, \end{cases} \tag{2.11}$$

where the minima are taken over all R with $1 < R < |\frac{2}{z} - 1|$.

We illustrate (2.11) for real $z = x$ and $a = 1.5$, $b = .5$, $c = 2.5$. In this case, the second line of (2.11) applies, and the kernel K_n is to be evaluated at $-R$, since $c > 2b$. Moreover, $\mu_R^-(x) = \frac{1}{2}(2 - x - R|x|)$, and the admissible values of R are $1 < R < 1 + \frac{2}{|x|}$ when $x < 0$, and $1 < R < \frac{2}{x} - 1$ when $0 < x < 1$. Table 2.1 shows the bounds (2.11) divided by $\gamma_0^J(b,c)|F(a,b;c;x)|$ or by $\gamma_0^J(b,c)$ (if $|F(a,b;c;x)|$ is larger resp. smaller than 1) for selected values of x and n.

x	$n=5$	$n=10$	$n=20$	$n=50$	$n=100$
.9	.22e+1	.70e–2	.36e–7	.11e–23	.11e–51
.6	.63e–4	.52e–10	.15e–22	.83e–61	.41e–125
.3	.27e–8	.21e–18	.54e–39	.18e–101	.41e–206
–1	.13e–5	.72e–13	.94e–28	.42e–73	.32e–149
–5	.12e–1	.50e–5	.37e–12	.36e–34	.22e–71
–10	.16e+0	.72e–3	.70e–8	.15e–23	.40e–50
–20	.11e+1	.28e–1	.93e–5	.91e–16	.14e–34
–50	.63e+1	.78e+0	.62e–2	.94e–9	.14e–20
–100	.15e+2	.42e+1	.17e+0	.34e–5	.19e–13

TABLE 2.1 Optimized error bounds for $a = 1.5$, $b = .5$, $c = 2.5$

As z approaches the imaginary axis, the radius R of the circle C_R approaches 1 and the computation of $K_n(\pm R)$ becomes more difficult. The use of elliptic contours would alleviate this problem somewhat; cf. the discussion in the next subsection.

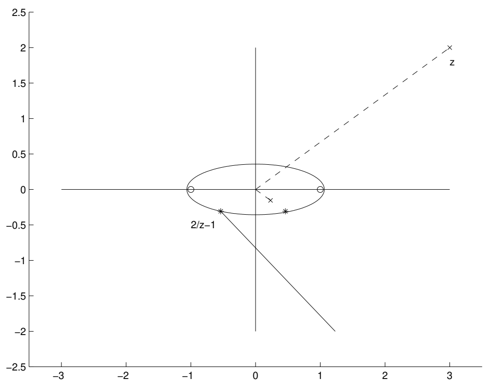

Figure 2.1. The limiting ellipse $\mathcal{E}_{\rho^*}$

2.3.2. *The case* $\operatorname{Re} z \geq 1$. Here, the cut of $\mathbb{C}_z^*$ intrudes into the unit disc, and we can no longer use circular contours Γ in (2.6). We use instead elliptic contours $\Gamma = \mathcal{E}_\rho$, $\rho > 1$, i.e., ellipses with foci ar ± 1 and sum of the semiaxes equal to ρ (cf. [7, §5]). The parameter ρ must be selected sufficiently small for $\mathcal{E}_\rho$ to avoid the cut. The limiting ellipse $\mathcal{E}_{\rho^*}$ is the one that passes through the end point $z^* = \frac{2}{z} - 1$ of the cut (see Fig.2.1).

To determine ρ^*, let $z^* = x^* + iy^*$. The ellipse $\mathcal{E}_\rho$ in parametric form is

$$\mathcal{E}_\rho = \{\zeta \in \mathbb{C} : \quad \zeta = \tfrac{1}{2}(\rho e^{i\theta} + \tfrac{1}{\rho}\, e^{-i\theta}),\ 0 \le \theta \le 2\pi\}. \tag{2.11}$$

In order for z^* to be on $\mathcal{E}_\rho$, we must have

$$\begin{aligned} \left(\rho + \frac{1}{\rho}\right)\cos\theta &= 2x^*, \\ \left(\rho - \frac{1}{\rho}\right)\sin\theta &= 2y^* \end{aligned}$$

for some θ, which implies

$$\frac{4x^{*2}}{\left(\rho + \frac{1}{\rho}\right)^2} + \frac{4y^{*2}}{\left(\rho - \frac{1}{\rho}\right)^2} = 1.$$

This amounts to an algebraic equation of degree 4 in ρ^2, namely

$$\begin{aligned} \rho^8 - 4(x^{*2} + y^{*2})\rho^6 + 2(4x^{*2} - 4y^{*2} - 1)\rho^4 \\ -4(x^{*2} + y^{*2})\rho^2 + 1 = 0. \end{aligned} \tag{2.12}$$

On geometric grounds, there must be a unique real root larger than 1. This root is the desired critical value ρ^* of the parameter ρ. The admissible elliptic contours Γ therefore are the confocal ellipses $\mathcal{E}_\rho$ with $1 < \rho < \rho^*$. If, as above, we write $z = 1 + re^{i\varphi}$, then $z^* = (1 - re^{i\varphi})/(1 + re^{i\varphi})$, i.e.,

$$x^* = -\frac{r^2 - 1}{r^2 + 2\cos\varphi + 1}, \quad y^* = -\frac{2\sin\varphi}{r^2 + 2\cos\varphi + 1}.$$

The real root $\rho^* > 1$ of (2.12) for these values of x^* and y^* is shown in Table 2.2 for selected values of r and φ.

r	$\varphi = \pi/2$	$\varphi = 3\pi/8$	$\varphi = \pi/4$
1	2.4142136	1.8708684	1.4966058
5	1.7968705	1.5535565	1.3409415
10	1.5395351	1.3923775	1.2506770
20	1.3645232	1.2727733	1.1787546
50	1.2197560	1.1680016	1.1123979
100	1.1513638	1.1167928	1.0788811

Table 2.2 Values of ρ^* for selected values of r and φ

Evidently, as φ decreases to 0, that is, z approaches the cut $[1, \infty]$, the value of ρ^* tends to 1, i.e., the ellipses $\mathcal{E}_{\rho^*}$ become progressively slimmer and degenerate to the interval $[-1, 1]$ in the limit. As a consequence, convergence of the quadrature rule slows down, as was observed experimentally in Fig. 2.2.

We now have from (2.6) that

$$E_n^J(a, b; c; z) = \frac{1}{2\pi i} \oint_{\mathcal{E}_\rho} K_n(\zeta) f^J(\zeta; z) d\zeta, \quad 1 < \rho < \rho^*. \tag{2.13}$$

To avoid the determination of $\max_{\zeta \in \mathcal{E}_\rho} |f^J(\zeta; z)|$, which is rather cumbersome, we estimate E_n^J as follows,

$$|E_n^J(a, b; c; z)| \leq \frac{1}{2\pi} \max_{\zeta \in \mathcal{E}_\rho} |K_n(\zeta)| \oint_{\mathcal{E}_\rho} |f^J(\zeta; z)||d\zeta|, \quad 1 < \rho < \rho^*. \tag{2.14}$$

Here, the integral on the right can be approximated by applying the composite trapezoidal rule to

$$\oint_{\mathcal{E}_\rho} |f^J(\zeta; z)||d\zeta| = \frac{1}{2} \int_0^{2\pi} |f^J(\zeta; z)| \sqrt{\rho^2 - 2\cos 2\theta + \rho^{-2}} d\theta \tag{2.15}$$

and the maximum of the kernel can be computed numerically.

As an illustration, we implemented this for $a = 1.5$, $b = .5$, $c = 2.5$, and for $z = 1 + re^{i\varphi}$ with the same values of r and φ as in Table 2.2. It is found,

r	$n=25$	$n=50$	$n=100$	$n=200$
1	.24e–15	.89e–32	.12e–64	.22 e–130
	.41e–10	.14e–21	.15e–44	.18e–90
	.16e–5	.85e–13	.25e–27	.22e–56
5	.53e–10	.10e–20	.39e–42	.58e–85
	.55e–7	.61e–15	.73e–31	.10e–62
	.66e–4	.38e–9	.13e–19	.14e–40
10	.29e–7	.47e–15	.12e–30	.84e–62
	.37e–5	.44e–11	.61e–23	.12e–46
	.78e–3	.84e–7	.96e–15	.13e–30
20	.31e–5	.86e–11	.66e–22	.39e–44
	.97e–4	.50e–8	.13e–16	.96e–34
	.48e–2	.60e–5	.93e–11	.23e–22
50	.16e–3	.50e–7	.46e–14	.39e–28
	.15e–2	.28e–5	.94e–11	.11e–21
	.24e–1	.33e–3	.59e–7	.20e–14
100	.95e–3	.31e–5	.34e–10	.40e–20
	.48e–2	.56e–4	.74e–8	.13e–15
	.48e–1	.24e–2	.52e–5	.25e–10

TABLE 2.3 Relative error bounds for the hypergeometric function $F(a,b;c;z)$, $a=1.5$, $b=.5$, $c=2.5$ and $z=re^{i\varphi}$, $\varphi=\pi/2,\ 3\pi/8,\ \pi/4$

in this case, that the maximum of $K_n(\zeta)$ in (2.14) is consistently attained at the left extreme point $-(\rho+1/\rho)$ of the ellipse $\mathcal{E}_\rho$. Moreover, using a composite trapezoidal rule on (2.15) with 100 subintervals is found to yield at least 2–3 correct decimal digits for all ρ not too close to ρ^*, specifically for $\rho=1+\lambda(\rho^*-1)$, $\lambda=.1(.1).8$. Invariably, the bound in (2.14) is found to decrease as λ increases through these values. In Table 2.3, we show the error bound in (2.14) for the ρ-value corresponding to $\lambda=.8$. The three vertical entries for each r and n correspond to the three values $\pi/2$, $3\pi/8$, and $\pi/4$ of φ. A true optimization of the bound over all $1<\rho<\rho^*$, similarly as was done in (1.19), is not feasible in this case, since the optimum seems to occur at a value of ρ very close to ρ^*, for which the numerical evaluation of the integral (2.15) becomes unreliable. Table 2.3 actually shows the error bound for $\rho=1+.8(\rho^*-1)$ divided by $\gamma_0^J(b,c)|F(a,b;c;z)|$ if $|F(a,b;c;z)|>1$, or divided by $\gamma_0^J(b,c)$ otherwise. This represents a bound on the relative resp. absolute error of the quadrature approximation to $F(a,b;c;z)$; cf. the discussion at the end of §1.4.

3. Concluding Remarks

It has been shown that Gaussian quadrature applied to the integral representation of confluent hypergeometric and hypergeometric functions is a powerful tool to evaluate these functions in large domains of the complex plane. An inherent limitation of this approach is the restriction of the parameters a, b, and c, if they are real, to satisfying the inequalities $b > a > 0$ resp. $c > b > 0$. The evaluation of these functions for other real values of the parameters can be accomplished, in principle, by using appropriate recurrence relations (see, e.g., [1, Eqs. **13.4.1**–**13.4.7** and **15.2.10**–**15.2.27**]). Complex values of the parameters are also accessible to our approach, but would require complex Gauss-Jacobi quadrature rules; see, e.g., Nuttal and Wherry [9], who use such rules in scattering theory, or Theocaris and Ioakimidis [10], who use them in elasticity theory. Further investigation of this would be interesting, but is beyond the scope of the present paper.

References

[1] Abramowitz, M. and Stegun, I.A. (Eds.) 1964. Handbook of mathematical functions with formulas, graphs, and mathematical tables. NBS Applied Mathematics Series, Vol. 55, U.S. Government Printing Office, Washington, D.C.

[2] Davis, P.J. and Rabinowitz, P. 1984. Methods of numerical integration, 2d ed., Academic Press, Orlando, FL.

[3] Donaldson, J.D. and Elliott, D. 1972. A unified approach to quadrature rules with asymptotic estimates of their remainders. *SIAM J. Numer. Anal. 9*, pp. 573–602.

[4] Elliott, D. 1971. Uniform asymptotic expansions of the Jacobi polynomials and an associated function. *Math. Comp. 25*, pp. 309–315.

[5] Gautschi, W. 1967. Computational aspects of three-term recurrence relations. *SIAM Rev. 9*, pp. 24–82.

[6] Gautschi, W. 1994. Algorithm 726: ORTHPOL — a package of routines for generating orthogonal polynomials and Gauss-type quadrature rules. *ACM Trans. Math. Software 20*, pp. 21–62.

[7] Gautschi, W. and Varga, R.S. 1983. Error bounds for Gaussian quadrature of analytic functions. *SIAM J. Numer. Anal. 20*, pp. 1170–1186.

[8] Karmazina, L.N. 1955. On a method of computation of the hypergeometric function (Russian). *Vyčisl. Mat. Vyčisl. Tehn. 2*, pp. 111–115.

[9] Nuttal, J. and Wherry, C.J. 1978. Gaussian integration for complex weight functions. *J. Inst. Math. Appl. 21*, pp. 165–170.

[10] Theocaris, P.S. and Ioakimidis, N.I. 1977. On the numerical solution of Cauchy type singular integral equations and the determination of stress intensity factors in case of complex singularities. *Z. Angew. Math. Phys. 28*, pp. 1085–1098.

Department of Computer Sciences
Purdue University
West Lafayette, IN 47907-1398, U.S.A.